

Svetlana Biza

Antiviral Drug Combinations for Treatment of Emerging and Re-emerging Viral Infections

Master's thesis in Molecular Medicine

Supervisor: Denis Kainov

May 2021

Svetlana Biza

Antiviral Drug Combinations for Treatment of Emerging and Re-emerging Viral Infections

Master's thesis in Molecular Medicine

Supervisor: Denis Kainov

May 2021

Norwegian University of Science and Technology

Faculty of Medicine and Health Sciences

Department of Clinical and Molecular Medicine



Norwegian University of
Science and Technology

Abstract

Today, combination antiviral therapy is one of the main methods of treatment of complex diseases, such as HIV, HCV and HBV. Antiviral drug combinations have advantages over monotherapies because of their greater efficacy, less toxicity, and their ability to combat coinfections or multiple viral agents at the same time. Moreover, monotherapy is more often associated with a high rate of viral drug resistance than treatment with multiple drugs.

In this thesis, we contribute to the development of combination antiviral therapy from two directions. First, we study novel antiviral combinations with synergistic effects against severe acute respiratory syndrome coronavirus 2 (SARS-CoV-2), hepatitis C virus (HCV), human immunodeficiency virus 1 (HIV-1) and echovirus 1 (EV1) *in vitro*. Secondly, we develop a database of antiviral drug combinations showing synergistic or additive effects against different types of human viruses.

As the result of the experimental work, we discovered that combinations of nelfinavir and convalescent serum, EIDD-2801, remdesivir, salinomycin, amodiaquine, homoharringtonine, or obatoclox showed synergistic activity against SARS-CoV-2 in human lung epithelial cells Calu-3, as well as a combination of amodiaquine plus salinomycin. We also detected that combinations of sofosbuvir plus brequinar or niclosamide are synergistic against HCV infection in Huh-7.5 cell culture. Also, we found that lamivudine-monensin and tenofovir-monensin combinations are synergistic against HIV-1 infection in human cervical TZM-bl cell line. In addition, we figured out that FDA-approved anti-cancer drug vemurafenib is an effective inhibitor of EV1. Finally, we observed synergistic antiviral activity of vemurafenib with emetine, homoharringtonine, anisomycin, or cycloheximide against EV1 infection in human lung epithelial A549 cells. These results reveal that a synergistic effect is achieved when an antiviral agent targeting a virus is combined with another compound targeting a virus or a host.

As the result of the development of antiviral drug combination database, we included almost 1000 antiviral combinations and covered 612 unique drugs and 68 different viruses and presented a detailed statistics of development stages of each drug combination. This database is aimed to significantly help researchers and experienced physicians to reduce time in identifying new promising combinations based on already conducted studies.

Acknowledgement

First and foremost, I would like to thank Dr. Denis Kainov for his indescribable support and assistance in this thesis process. His passion for virology deeply inspired me. I would also like to thank him for his professionalism and a great sense of humor. I am eternally grateful for everything that I have learned from you.

Further, I want to say thank my colleagues for the wonderful collaboration. This project would have been impossible without your support and knowledge.

Finally, I want to say a special thank to my husband. Thank you for always being by my side, guiding me through tough situations and always helping me.

Thank you all,
Svetlana Biza

Publications

The work that has been conducted in this thesis resulted in being a part of two scientific publications that have been officially published in *Viruses*. The publication references are provided below:

1. Ianevski, A., et al., *Potential Antiviral Options against SARS-CoV-2 Infection*. *Viruses*, 2020, 12(6): p. 642.
2. Ianevski, A., et al., *Identification and Tracking of Antiviral Drug Combinations*. *Viruses*, 2020, 12(10).

Table of Contents

Chapter 1 Introduction.....	1
Chapter 2 Methodology	5
2.1 Experimental search for antiviral drug combinations	5
2.1.1 Drugs	5
2.1.2 Cell cultures	5
2.1.3 Viruses	6
2.1.4 Drug test.....	6
2.1.5 Virus quantification.....	7
2.1.6 Drug Combination Test and Synergy Calculations	7
2.1.7 Gene Expression Profiling	8
2.1.8 Cytokine Analysis	8
2.1.9 Metabolic Analysis.....	9
2.2 Database development	10
Chapter 3 Results and Discussion	13
3.1 Experimental search for new antiviral drug combinations	13
3.1.1 Novel Drug Combinations against SARS-CoV-2 infection in vitro	13
3.1.2 Novel drug combinations against HCV infection in vitro	16
3.1.3 Antiviral drug Combinations against HIV-1 infection.....	19
3.1.4 Novel antiviral drug combinations against EV1	21
3.2 Results on the development of drug combination database	27
Chapter 4 Conclusions and Future Work.....	29
4.1 Conclusions	29
4.2 Future work	30
References	31
Appendix A – Drugs’ description used in experimental work	35
Appendix B – Antiviral drug combinations database	40

Abbreviations

BSAA(s)	Broad-spectrum antiviral agent(s)
BSL-3	Biological Safety Level 3
BSA	Bovine serum albumin
Calu-3	Cultured Human Airway Epithelial Cells
CC50	The half-maximal cytotoxic concentration
ChiCTR	Chinese Clinical Trial Registry
CTG	Cell Titer Glow
DMSO	Dimethyl sulfoxide
DMEM	Dulbecco's Modified Eagle Medium
ESI	Electrospray ionization
EBOV	Ebola virus
EV1 (6)	Echovirus 1 (6)
EC50	The half-maximal effective concentration
FDA	United States Food and Drug Administration
HIV	Human immunodeficiency virus
HCV	Hepatitis C virus
HBV	Hepatitis B virus
Hpi	Hour(s) post infection
IFN	Interferon
MoH	Ministry of Health
MERS-CoV	Middle East respiratory syndrome coronavirus
NEAA	Non-essential amino acid
PD	Pharmacodynamics
PK	Pharmacokinetics
SARS-CoV-2	Severe acute respiratory syndrome coronavirus-2
SARS-CoV	Severe acute respiratory syndrome coronavirus
SI	Selectivity index
VGM	Virus growth medium
WHO	World Health Organization
ZIP model	Zero-interaction potency model

Chapter 1

Introduction

Since the beginning of the human era, viral diseases have caused the death of millions of people around the world that required the development of effective antiviral therapy.

The first scientist who reached noticeable achievements against viral infections was William Prusov. He synthesized the first antiviral drug, idoxuridine, which was approved as an effective drug against herpes simplex virus in mid-1963 (Bauer 1985). This promising discovery was the starting point when we got effective solutions against certain viruses which we developed significantly over the years. By 2016, the number of officially approved antiviral drugs for the treatment of HIV, HBV and HCV, herpes virus, influenza virus, human cytomegalovirus, chickenpox virus, respiratory syncytial virus and human papillomavirus infections increased to 90 (De Clercq and Li 2016).

One of the main challenges to our armamentarium of antiviral drugs is the emergence of resistant mutants. Viral strains have developed resistance to common antiviral drugs, especially for antiviral monotherapy (Irwin et al. 2016). For this reason, combinations of antiviral agents became a promising advancement in the fight against severe viruses.

Combination drug therapies are established as the treatment standard against rapidly mutating viruses such as HIV and HCV (Naggie and Muir 2017; Ghosn et al. 2018; Chaudhuri, Symons, and Deval 2018). For instance, antiretroviral medicines such as Truvada (emtricitabine/tenofovir disoproxil fumarate), Epsicom (abacavir/lamivudine), and Kaletra (lopinavir/ritonavir) contain cocktails of antiviral drugs that effectively suppress the replication of the virus in the host's body (<https://www.drugs.com/condition/hiv-infection.html>). Similarly, elbasvir/grazoprevir and sofosbuvir/velpatasvir combinations are important components in the treatment of HCV infection (<https://www.drugs.com/condition/chronic-hepatitis-c.html>).

The use of antiviral drug combinations has significant advantages over monotherapy for several reasons. First, combination therapy prevents or forestalls the development of drug resistance by fighting against viruses through various mechanisms simultaneously (Nijhuis, van Maarseveen, and Boucher 2009). In addition, combination antiviral therapy minimizes toxicity by reducing individual drug dosages that reduces the likelihood of side effects. Moreover, combinations that show additive or synergistic activity increase the effectiveness of treatment by increasing the overall antiviral activity against viral diseases (Ianevski, Yao, Biza, et al. 2020).

The second biggest challenges in usage of antiviral drugs is the emergence of poorly characterized viruses and the re-emergence of infections (Woolhouse et al. 2012). In this case, the production of new antiviral molecules is an energy-intensive, time-consuming and expensive process, and the use of antiviral monotherapy is not always effective (Bekerman and Einav 2015). There are two main strategy to solve this problem: drug redirecting and combination therapy (Andersen et al. 2020; Ianevski, Yao, Biza, et al. 2020; García-Serradilla, Risco, and Pacheco 2019). Drug redirecting allows to gain additional value from an existing drug by targeting a disease other than the one for which it was originally created (Adalja and Inglesby 2019; Andersen et al. 2020). In contrast, combinations of antiviral drugs is promising against poorly characterized viruses because different classes of drugs can affect different stages of the viral replication cycle at the same time that results in greater efficiency (Govorkova and Webster 2010; Melville, Rodriguez, and Dobrovolny 2018). In addition, it helps to save time and money to skip not only preclinical stages (in vitro and in vivo), but also the first stage (bioequivalence stage) of clinical trials.

In some cases, emerging or re-emerging viruses can appear and spread from natural reservoirs, infecting people with varying degrees of damage, up to death. Unfortunately, 2019 was not an exception and SARS-CoV-2 infection has emerged as a serious global health threat. Various strategies are currently being used to treat this dangerous virus, and antiviral drug combinations have proven to be a promising and innovative therapy (Siddiqui et al. 2020). Many different drug combinations are currently undergoing clinical trials against SARS-CoV-2 (NCT04252885, NCT04291729, NCT04304053, etc.).

As we see, the usage of antiviral drugs combinations against viral infections has several advantages over monotherapy. However, there is lack of a systematic summary of the tested drug combinations that are reported in the literature. Creating such an information resource that

will contain all possible antiviral drugs that show additive or synergistic activity at different stages (in vitro, in vivo and in clinical trials). The information contained in such a database can significantly help researchers and experienced physicians to reduce time in identifying new promising combinations based on already conducted studies. As such, as the first main contribution of this thesis, we created a centralized database which contains more than 1000 antiviral compound combinations at different stage of development against 54 types of viruses.

In addition, there is a strong need in searching for new combinations of antiviral drugs for the treatment and control of HIV, HCV, SARS-CoV-2 and EV1 infections because we are still facing problems in fighting with these viruses and the current treatment is still not sufficient (McCluskey, Siedner, and Marconi 2019; Loggi, Vukotic, and Andreone 2018; Ali and Alharbi 2020). As such, the second main contribution of this work is experimental studies and analysis of novel synergistic combinations against HIV, HCV, SARS-CoV-2 and EV1 diseases. Overall, we tested 43 combinations of antiviral compounds and found 17 promising combinations.

Chapter 2

Methodology

2.1 Experimental search for antiviral drug combinations

In this section, the main tools, supply materials, used drugs and tested viruses are described.

2.1.1 Drugs

Table A1 lists compounds used in experiments, their suppliers, and catalogue numbers. Table A2 contains chemical structure (2D or 3D) of these compounds taken from open chemistry database - PubChem. To obtain 10 mM stock solutions, compounds were dissolved in dimethyl sulfoxide (DMSO; Sigma-Aldrich, Hamburg, Germany) or milli-Q water. The solutions were stored at $-80\text{ }^{\circ}\text{C}$ until use. A convalescent serum sample from a recovered patient with SARS-CoV-2 was isolated for the clinical trial (NCT04320732; REK: 124170) and provided for this research experiment (Ianevski, Yao, Fenstad, et al. 2020).

2.1.2 Cell cultures

Human telomerase reverse transcriptase-immortalized retinal pigment epithelial (RPE) and non-small-cell lung cancer Calu-3 cell cultures were grown in DMEM-F12 added with 100 $\mu\text{g}/\text{mL}$ streptomycin, 10% FBS, and 100 U/mL penicillin (Pen–Strep). Vero-E6 and human adenocarcinoma alveolar basal epithelial A549 cells were grown in DMEM supplemented with 10% FBS and Pen–Strep. The cell cultures were kept stored $37\text{ }^{\circ}\text{C}$ in the presence of 5% CO_2 . TZM-bl is a human cervical cancer HeLa cell line, stably expressing the firefly luciferase under control of the HIV-1 LTR promoter. TZM-bl cell line was grown in DMEM added with 10% FBS and Pen/Strep. ACH-2 cells have a single integrated copy of the provirus HIV-1 strain LAI (NIH AIDS Reagent Program). This cell line was grown in RPMI-1640 medium added

with 10% FBS and Pen–Strep. The human hepatoma Huh-7.5 cells were grown in DMEM added with 10% FBS, NEAA, L-glutamine and Pen–Strep (Lee et al. 2016). All cells were grown at 37 °C with 5% CO₂.

2.1.3 Viruses

The seven SARS-CoV-2 strains (hCoV-19/Norway/Trondheim-E10/2020, hCoV-19/Norway/Trondheim-E9/2020, hCoV-19/Norway/Trondheim-S15/2020, hCoV-19/Norway/Trondheim-S12/2020, hCoV-19/Norway/Trondheim-S10/2020, hCoV-19/Norway/Trondheim-S5/2020, hCoV-19/Norway/Trondheim-S4/2020) were isolated under a Biological Safety Level 3 (BSL-3) facility and provided for these experiments (Ianevski, Yao, Fenstad, et al. 2020). ACH-2 cell line was seeded in 10 mL medium to make HIV-1, 6×10^6 . In addition, 100 nM phorbol-12-myristate-13-acetate was added to induce virus production. The HIV-1-containing medium was collected after 48 h. Using anti-p24-ELISA, which was developed in-house, the amount of HIV-1 was estimated by measuring the concentration of HIV-1 p24 in the medium. Recombinant purified p24 protein was used as a reference. Echovirus 1 (Farouk strain; ATCC) was provided by Prof. Marjomäki from University of Jyväskylä. EV6 was isolated earlier and provided for this experiment (Smura et al. 2013). EV1 and EV6 viruses were amplified in a monolayer of A549 cell line in the DMEM media including 0.2% BSA and Pen–Strep. The human hepatoma Huh-7.5 cell line transiently transfected with HCV RNA transcripts of a cell culture-adapted JFH1 genome expressing NS5A-GFP fusion protein (JFH1_5A/5B_GFP). After 4 days, HCV cells were harvested including medium. Further, viral supernatant was clarified by filtration using a syringe filter with a 0.2 µm pore size (Millipore, Bedford, MA, USA). All virus stocks were stored at -80 °C.

2.1.4 Drug test

Approximately 4×10^4 Vero-E6, RPE or A549 cells were seeded per well in 96-well plates. The cell cultures were grown for 24 h in DMEM or DMEM-F12 added with Pen–Strep and 10% FBS. The medium was replaced with DMEM or DMEM-F12 containing 0.2% BSA and Pen–Strep. The viral compounds were added to the cell lines in 3-fold dilutions at 7 different concentrations, starting from 30 µM. No compounds were added to the control wells. The cell cultures were mock- or virus-infected at a moi of 0.1. After 72 h for SARS-CoV-2 and 24 h for

EV1, the medium was extracted from the cell lines. CellTiter-Glo assay was performed to measure the viability of cells.

The CC50 for each compound was calculated based on viability/death curves obtained on mock-infected cells after nonlinear regression analysis with a variable slope using GraphPad Prism software version 7.0a (GraphPad Software, San Diego, CA, USA). The EC50 were calculated based on the analysis of the viability of infected cells by fitting drug dose–response curves using the four-parameter (4PL) logistic function $f(x)$:

$$f(x) = A_{min} + \frac{A_{max} - A_{min}}{1 + \left(\frac{x}{m}\right)^\lambda}$$

Where $f(x)$ denotes a response value at dose x , A_{max} and A_{min} - the upper and lower asymptotes (minimal and maximal drug effects) respectively, m - the dose that produces the EC50 or CC50, and λ - the steepness (slope) of the curve. The relative effectiveness of the drug was defined as the selectivity index (SI = CC50/EC50).

2.1.5 Virus quantification

Media from a viral cell line were serially diluted from 10^{-2} to 10^{-7} in serum-free media containing 0.2% BSA. The dilutions were applied to a monolayer of Vero-E6 (for SARS-CoV-2) or A549 (for EV1) cells in 24-well plates. After 1 h, cells were overlaid with virus growth medium containing 1% carboxymethyl cellulose and incubated for 72 (for SARS-CoV-2) or 48 h (for EV1). The cells were fixed and stained with crystal violet dye, and the plaques were calculated in each well and expressed as plaque-forming units per mL (pfu/mL).

2.1.6 Drug Combination Test and Synergy Calculations

A549 cell culture was treated with different concentrations of two drugs and infected with EV1 (moi 0.1) or mock. Cell viability was measured using CellTiter-Glo after 24h. Vero-E6 cell line was treated with different concentrations of two antiviral compounds and infected with SARS-CoV-2 (moi 0.1) or mock. Cell viability was measured using CellTiter-Glo after 72h. TZM-bl cell culture was treated with different concentrations of two drugs and infected with HIV-1 (corresponding to 300 ng/mL of HIV-1 p24) or mock. The media was extracted from the cells via 48 hpi, the cells were lysed, and firefly luciferase activity was measured using the luciferase assay system (Promega, Madison, WI, USA).

In a parallel experiment, cell viability was measured using CellTiter-Glo. In addition, toxicity and antiviral activity of drug combinations were examined using GFP-expressing HCV in Huh-7.5 cells by following described procedures (Lee et al. 2017).

To test whether the drug combinations act synergistically, the observed responses were compared with expected combination responses. The expected responses were calculated based on the ZIP reference model using SynergyFinder version 2 (Ianevski et al. 2017; Ianevski, Giri, and Aittokallio 2020). We quantified synergy scores, which represent the average excess response due to drug interactions (i.e., 10% of cell survival beyond the expected additivity between single drugs has a synergy score of 5).

2.1.7 Gene Expression Profiling

A549 cell culture was treated with 10 μ M vemurafenib or vehicle at indicated concentrations. Cells were infected with EV1 at moi 0.1 or mock. RNA was extracted after 8h using RNeasy Plus Mini kit (Qiagen, Hilden, Germany). Gene expression analysis was performed using Human HT-12 v4 Expression BeadChip Kit (Illumina, San Diego, CA, USA) according to the manufacturer's recommendation.

Raw microarray data were normalized using the BeadArray and Limma packages from Bioconductor suite for R (Ritchie et al. 2015). Normalized data were further processed using variance and intensity filter. Genes differentially expressed between samples and controls were determined using the Limma package. The Benjamini–Hocberg method was used to filter out differentially expressed genes based on a q-value threshold ($q < 0.05$). Filtered data were picked out by logarithmic fold change (\log_2FC). Heatmap was generated using an in-house developed interface, Breeze (Potdar et al. 2020). Gene set enrichment analysis was done through open-source software (www.broadinstitute.org/gsea).

2.1.8 Cytokine Analysis

After 24 hpi, the medium from EV1- or mock-infected, non- or drug-treated A549 cell line was collected and clarified by centrifugation for 5 min at 14,000 rpm. Cytokine profiling was analyzed using Proteome Profiler Human Cytokine Array Kit (R&D Systems, Abingdon, UK) according to the instructions provided.

2.1.9 Metabolic Analysis

Ten microliters of labeled internal standard mixture was added to 100 μ L of the sample (cell culture media). Further, 0.4 mL of solvent (99% ACN and 1% FA) was added to each sample. The insoluble fraction was removed by centrifugation for 14,000 rpm, 15 min, and 4 °C. The collected extracts were dispensed in Ostro™ 96-well plate (Waters Corporation, Milford, MA, USA) and filtered by applying vacuum at a delta pressure of 300–400 mbar for 2.5 min on robot's vacuum station. The clean extract was collected to a 96-well collection plate, placed under the Ostro™ plate. The collection plate was sealed and centrifuged for 15 min, 4000 rpm, 4°C, and placed in autosampler of the liquid chromatography system for the injection. Sample analysis was performed on an Acquity UPLC-MS/MS system (Waters Corporation, Milford, MA, USA). The autosampler was used to perform partial loop with needle overflow injections for the samples and standards. The detection system, a Xevo TQ-S tandem triple quadrupole mass spectrometer (Waters, Milford, MA, USA), was operated in both positive and negative polarities with a polarity switching time of 20 ms. ESI was chosen as the ionization mode with a capillary voltage at 0.6 KV in both polarities. The source temperature and desolvation temperature of 120°C and 650°C, respectively, were maintained constant throughout the experiment.

Declustering potential (DP) and collision energy (CE) were optimized for each compound. Multiple reaction monitoring (MRM) acquisition mode was selected for quantification of metabolites with individual span time of 0.1 s given in their individual MRM channels. The dwell time was calculated automatically by the software based on the region of the retention time window, number of MRM functions and also depending on the number of data points required to form the peak. MassLynx 4.1 software was used for data acquisition, data handling, and instrument control (Agilent, Santa Clara, CA, USA).

Data processing was done using TargetLynx software (Agilent, Santa Clara, CA, USA), and metabolites were quantified by calculating curve area ratio using labeled internal standards (IS) (area of metabolites/area of IS) and external calibration curves. Metabolomics data were log₂ transformed for linear modeling and empirical-Bayes-moderated t-tests using the LIMMA package (<https://bioconductor.org/packages/release/bioc/html/limma.html>). To analyze the differences in metabolite levels, a linear model was fit for each metabolite. The Benjamini–Hochberg method was used to correct for multiple testing. The significant metabolites were determined at a Benjamini–Hochberg false discovery rate (FDR) controlled at 10%. The

heatmap was generated using the pheatmap package (<https://cran.rproject.org/web/packages/pheatmap/index.html>) based on log-transformed profiling data. MataboAnalyst 3.0 was used to identify pathways related to EV1 infection (www.msea.ca). In this pathway analysis tool, the pathway data are derived from KEGG database (www.genome.jp/kegg/).

2.2 Database development

To develop an extensive database that contains all possible combinations of antiviral drugs with additive or synergistic activity, we did a comprehensive literature search. We went through thousands of articles from PubMed, Web on Science, Scopus, Google scholar as well as other public sources to extract literature-supported antiviral combinations. We have used and analyzed not only original research manuscripts, review articles, but also case reports that cover any aspect of antiviral drug combinations and related topics. In addition, we reviewed the references of retrieved articles to identify additional studies not retrieved by the initial search. To find antiviral combinations that are in different stages (I-IV) of clinical trials, we used ClinicalTrials.gov website, which collects data from clinical trials from around the world, Chinese Clinical Trial Registry (ChiCTR), official register of clinical trials of the Ministry of Health (MoH) of Russia and EU Clinical Trials Register.

To find necessary information we used the following keyword combinations:

#1: "Synergistic" OR "Antiviral" OR "Additive" OR "Combinatorial"

AND

#2: "Drug Therapy" OR "Drug combinations" OR "Combination drug therapy" OR "Combinations"

In addition, to find combinations of drugs for specific viruses, we added the names of the viruses after the keywords (the virus is provided as an example):

AND

#3: "Severe acute respiratory syndrome coronavirus 2" OR "SARS-CoV-2" OR "COVID-19"

Also, to make the database more comprehensive and detailed, we used PubChem, AdisInsight, Drugs.com, DrugBank, DrugCentral2020 as well as other public sources where I could find

primary indications of antivirals (experimental, investigational or approved) and potential targets, which these drugs use to fight with different viruses.

To structure the collected information, we created an Excel document with an antiviral drug combinations table which is attached to this thesis as a separate document. In Figure 1, the overview of the table structure and its headings is provided. There are seven main columns: antiviral drug combinations, primary indications of compounds, stage of combination, type of virus, potential target, main reference, and extra reference. The first column includes names of antivirals used in a combination cocktail. The second section has three levels of primary indications of drugs (experimental, investigational,

and approved). Next, the stage of combination column represents the stage of development of antiviral combinations (in vitro, in vivo or in clinical trials). The fourth section contains the abbreviated name of the virus against which drug combinations act. More information about the viruses included in the fourth column is shown in Table B1, such as full names, which family they belong to, which structure of the genetic material they have, and what diseases they can cause. The fifth column indicates a potential target which each antiviral compound used (e.g. Viral RNA pol, Viral DNA pol, IFNAR). Finally, the last two columns contain special identifiers to make it easier to find the information included in the table for the respective drug combination.

Antiviral Drug combinations			Primary indications			Stage of combination			Virus	Potential target			Reference I	Reference II
Drug I	Drug II	Drug III	Drug I	Drug II	Drug III	In vitro	In vivo	Clinical trials		Drug I	Drug II	Drug III		

Figure 1 - The structure of the headers of the anti-virus combinations table

Chapter 3

Results and Discussion

3.1 Experimental search for new antiviral drug combinations

3.1.1 Novel Drug Combinations against SARS-CoV-2 infection in vitro

According to the World Health Organization (WHO), by the end of February 2021, the number of people affected by SARS-CoV-2 reached 110.7 million cases in the world and over 2.4 million deaths since the start of the pandemic (WHO 2021).

Unfortunately, these numbers continue to grow day by day, so we need more solutions to control SARS-CoV-2 infection.

3.1.1a Experiment with G614 and nelfinavir

As a promising compound combination against SARS-CoV-2, a convalescent serum sample from recovered patient (G614) was tested in a combination with nelfinavir in human lung epithelial Calu-3 cells (Figure 2). G614 was selected for experimental testing within this combination because G614 neutralized the SARS-CoV-2 virus and prevented the virus-mediated death of Vero-E6 cells (Ianevski, Yao, Fenstad, et al. 2020). At the same time, nelfinavir, which is an approved antiretroviral protease inhibitor that is used in the HIV therapy, has been demonstrated to inhibit SARS-CoV-2 in vitro (Ianevski, Yao, Fenstad, et al. 2020; Musarrat et al. 2020; Xie et al. 2020). In addition, there was a case report where nelfinavir has shown promising results in treatment of patients with SARS-CoV-2 infection (<https://www.researchsquare.com/article/rs-27346/v1>).

The combination of G614 and nelfinavir displayed synergy antiviral SARS-CoV-2 activity with synergy score: 13 (Table 1). It is worth noting that at selected concentrations, nelfinavir

and G614 serum combination decreased the virus production by > 2 logs in comparison to nelfinavir alone (Figure 2).

	Efficacy (Zip score)	Selectivity (Zip score)
Nelfinavir + G614	12.65	13.21
Nelfinavir + Remdesivir	11.18	5.96
Nelfinavir + EIDD-2801	17.45	13.72

Table 1 - Synergy score for three drug combinations, which were calculated for Efficacy (SARS-COV-2 infected) and for Selectivity (SARS-CoV-2-infected-mock-infected) dose response matrices.

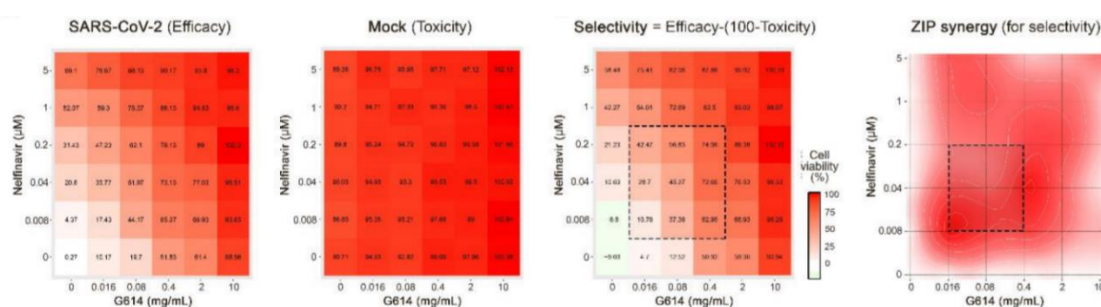


Figure 2 - Landscape of the interaction of convalescent serum with nelfinavir on Calu-3 cells -mock or -infected with SARS-CoV-2 (modified from (Ianevski, Yao, Biza, et al. 2020)).

3.1.1b Experiment with GS-5734 and nelfinavir

In the second drug combination experiment, remdesivir (GS-5734) was the next antiviral drug of choice for combination with nelfinavir. Remdesivir is an investigational antiviral, which showed antiviral activities against Ebola virus (EBOV) in phase II-III of a clinical trial (NCT03719586). In addition, remdesivir has antiviral activities against SARS-CoV in animal models and against MERS-CoV in vitro studies (Sheahan et al. 2017). Moreover, remdesivir showed antiviral activities against SARS-CoV-2, human CoVs OC43 (HCoV-OC43) and 229E (HCoV-229E) in vitro (Brown et al. 2019; Ianevski, Yao, Fenstad, et al. 2020).

Nelfinavir in combination with remdesivir reached synergistic effect in Calu-3 cell culture with synergy scores 6 against SARS-CoV-2 (Table 1).

3.1.1c Experiment with EIDD-2801 and nelfinavir

Next, we tested combinations of the antiretroviral protease inhibitor nelfinavir with EIDD-2801. EIDD-2801 is designed as a prodrug of N4-Hydroxycytidine (NHC) and has a broad-

spectrum anti-influenza efficacy (Toots et al. 2019). Moreover, EIDD-2801 was active against SARS-CoV-2 in vitro, in vivo and is participating in phase II of clinical trials against COVID-19 infection NCT04405570 (Ianevski, Yao, Fenstad, et al. 2020; Plemper, Cox, and Wolf 2020).

Combination of nelfinavir and EIDD-2801 showed synergistic effect with synergy score 14 (Table 1).

3.1.1d Experiment with cycloheximide/cepharanthine and nelfinavir

Next, we tested combinations of nelfinavir and cycloheximide or cepharanthine in vitro against SARS-CoV-2. Cycloheximide is a protein synthesis inhibitor produced by the bacterium *Streptomyces griseus*. Cycloheximide showed antiviral activities against human coronavirus OC43 (HCoV-OC43), human coronavirus NL63 (HCoV-NL63), Middle East respiratory syndrome coronavirus (MERS-CoV), murine coronavirus (strain A59) (MHV-A59) (Khalifa et al. 2020). In addition, cycloheximide has prevented the SARS-CoV-2-mediated death of Vero-E6 cells (Ianevski, Yao, Fenstad, et al. 2020). Cepharanthine is a naturally occurring alkaloid isolated from *Stephania*. This alkaloid has antiviral effects against various coronaviruses. Cepharanthine has shown its antiviral activity against HCoV-OC43 and SARS-CoV in vitro (Zhang et al. 2005; Kim et al. 2019). In addition, cepharanthine was confirmed to be active against SARS-CoV-2 on Vero-E6 cells (Ianevski, Yao, Fenstad, et al. 2020).

Unfortunately, synergy effect of nelfinavir and cycloheximide or cepharanthine was achieved at cytotoxic concentrations against SARS-CoV-2 in Calu-3 cells.

3.1.1e Experiment with nelfinavir, salinomycin, amodiaquine, homoharringtonine, obatoclax and emetine

To find more effective drug combinations against the COVID-19 infection in vitro, we used the following BSAAs in different combinations: nelfinavir, salinomycin, amodiaquine, homoharringtonine, obatoclax and emetine. These six compounds showed anti-SARS-CoV-2 activities in Vero-E6 cell line (Ianevski, Yao, Fenstad, et al. 2020). Fifteen antiviral combinations of the above drugs were tested. Cells were treated with varying concentrations of a two-drug combination and monitored the cell viability (Figure 3).

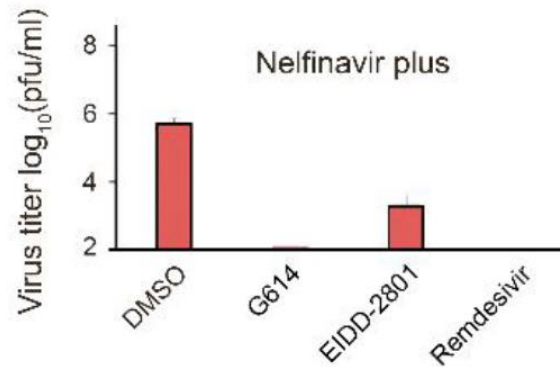


Figure 3 - Plaque reduction assay was used to measure the effects of nelfinavir plus DMSO, G614, EIDD- 2801 or Remdesivir on SAR-CoV-2 replication (modified from (Ianevski, Yao, Biza, et al. 2020)).

The observed drug combination responses were compared with the expected combination responses calculated by means of the ZIP model (Ianevski, Giri, and Aittokallio 2020; Ianevski et al. 2017). We quantified synergy scores, which represent the average excess response due to drug interactions (i.e. 10% of cell survival beyond the expected additivity between single drugs has a synergy score of 10). Combinations of nelfinavir with salinomycin, amodiaquine, homoharringtonine and obatoclox, as well as the combination of amodiaquine and salinomycin, were synergistic (most synergistic area assessment more than 10) (Figure 4). Moreover, the amodiaquine - nelfinavir combination was effective against 7 different strains of SARS-CoV-2 infection: S4, S5, S10, S12, S15, E9 and E10 (Figure 5).

3.1.If Conclusions on drug combinations against SARS-CoV-2 infection in vitro

From all the experiments described above, it can be concluded that the nelfinavir-convalescent serum G614, nelfinavir-EIDD-2801, nelfinavir-remdesivir, nelfinavir-salinomycin, nelfinavir-amodiaquine, nelfinavir-homoharringtonine, nelfinavir-obatoclox and amodiaquine-salinomycin combinations could result in better efficacy and decreased toxicity for the treatment of SARS-CoV-2 than these drugs alone.

3.1.2 Novel drug combinations against HCV infection in vitro

According to the WHO, hepatitis C caused by the hepatitis C virus (HCV) is the leading cause of cirrhosis and liver cancer (WHO 2020). Unfortunately, there is no protective vaccine against HCV and treatment options are still limited, so we need to develop an additional antiviral protection (Bailey, Barnes, and Cox 2019; Loggi, Vukotic, and Andreone 2018).

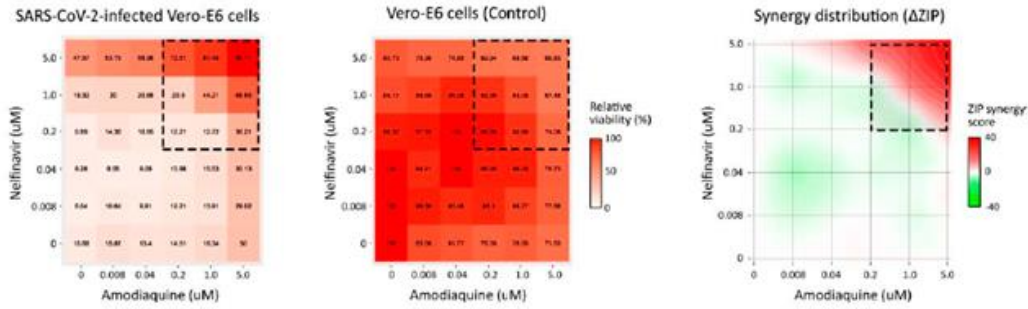


Figure 4 - Landscape of the interaction of nelfinavir plus amodiaquine on Vero-E6 cells - mock or -infected with SARS-CoV-2 (modified from (Ianevski, Yao, Fenstad, et al. 2020)).

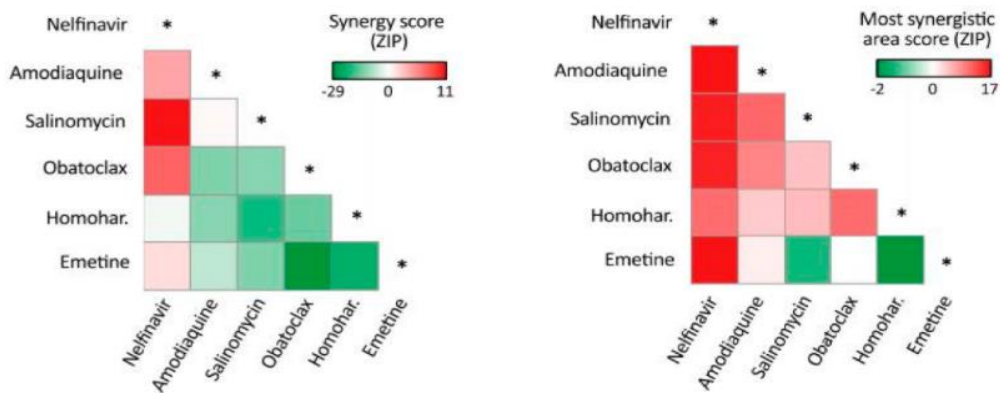


Figure 5 - Interaction of 15 drug combinations. Left panel depicts synergy scores; Right panel shows the most synergistic area scores of 15 drug combinations (modified from (Ianevski, Yao, Fenstad, et al. 2020)).

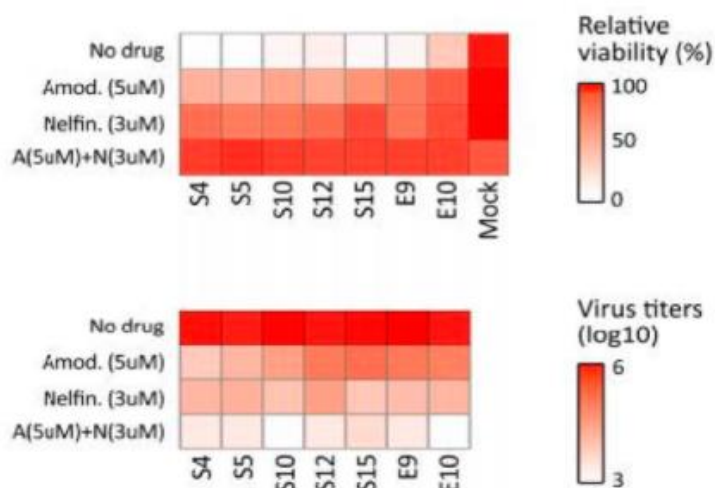


Figure 6 - Upper panel depicts viability of cells infected with 7 different strains of SARS-CoV-2 infection. Lower panel shows effects of the amodiaquine-nelfinavir combination on viral replication (modified from (Ianevski, Yao, Fenstad, et al. 2020)).

Through a review of different articles, we have identified several potential compounds that may have a synergistic effect in combination against HCV in vitro (Andersen et al. 2020; Bösl et al. 2019; Ianevski et al. 2019).

Four pair of drug combinations were tested: sofosbuvir plus brequinar, emetine, homoharringtonine or niclosamide using HCV-GFP chimera virus in Huh-7.5 cells (Bösl et al. 2019). Virus- and mock-infected Huh-7.5 cells were treated with an increasing concentration of two drugs. Each drug in a combination was added to the cells at 8 different concentrations starting from 0 μM (0 μM ; 0, 0156 μM ; 0, 031 μM ; 0, 06 μM ; 0,125 μM ; 0, 25 μM ; 0, 5 μM ; 1 μM). After 48 h of infection, HCV-mediated GFP expression was measured to determine compound efficiency of drug combinations against HCV infection. Together with this, cell viability was measured in mock-infected Huh-7.5 cells using CTG assay to determine combinations toxicity.

Through the experimental results we observed that only two drug combinations which are sofosbuvir-brequinar (Figure 6) and sofosbuvir-niclosamide (Figure 7) decreased GFP expression with synergy scores of 24 and 5, respectively.

Thus, it can be concluded that the sofosbuvir-brequinar and sofosbuvir-niclosamide combinations could result in better efficacy and decreased toxicity for the treatment of HCV infection than these drugs alone.

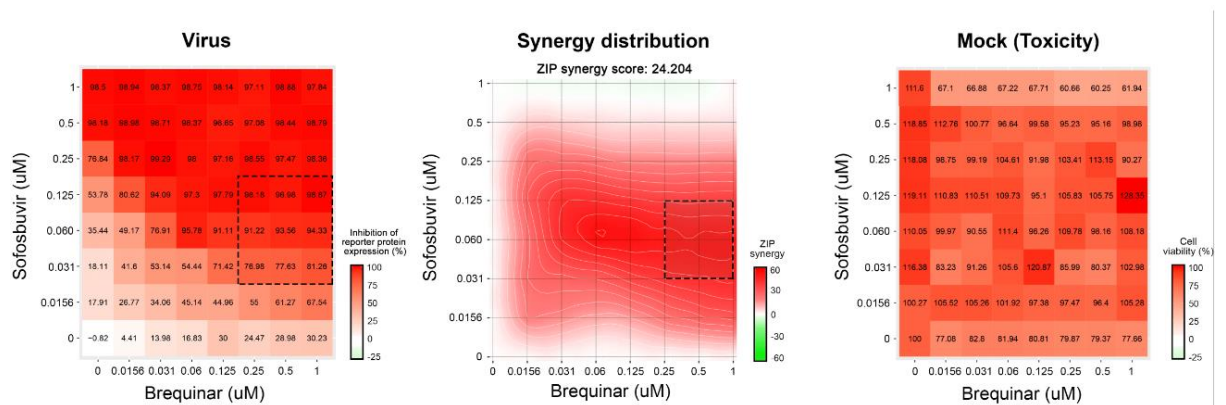


Figure 7 - Sofosbuvir and Brequinar combination landscape. This combination inhibits GFP-expressing HCV in Huh-7.5 cell culture. The left panel shows interaction of two drugs measured by GFP-expressing HCV. The right panel depicts interaction of Sofosbuvir with Brequinar, measured by CTG assay on mock-infected line (modified from (Ianevski, Yao, Biza, et al. 2020)).

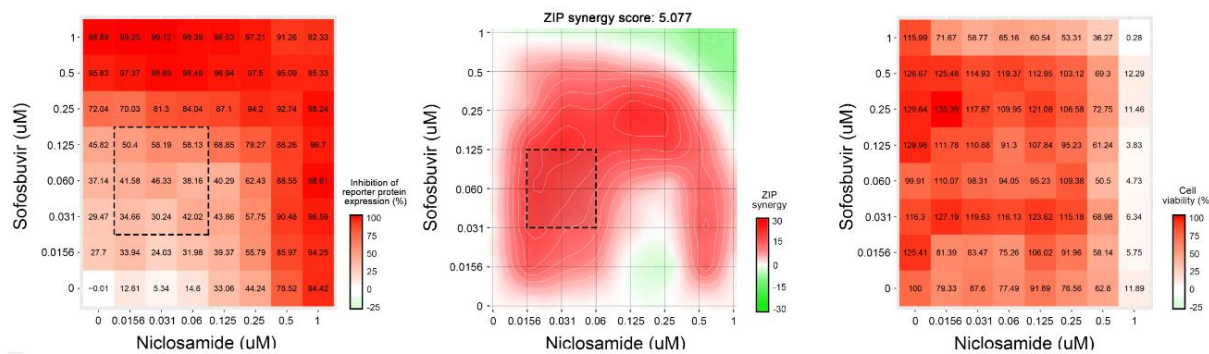


Figure 8 - Sofosbuvir and Niclosamide combination landscape. This combination inhibits GFP-expressing HCV in Huh-7.5 cell culture. The left panel shows interaction of two drugs measured by GFP-expressing HCV. The right panel depicts of Sofosbuvir with Niclosamide interaction measured by CTG assay on mock-infected cell culture (modified from (Ianevski, Yao, Biza, et al. 2020)).

3.1.3 Antiviral drug Combinations against HIV-1 infection

According to the WHO, at the end of 2019, there were approximately 38 million people living with HIV worldwide (WHO 2019).

There is no effective vaccine against HIV infection to protect people, but antiretroviral therapy is available. Effective antiretroviral treatment helps to reduce mortality and improve the quality of life of these patients. Moreover, to achieve effective control over this virus, it is necessary to use antiviral combinations, which have become the standard of therapy (Saag 2019). For this reason, new combinations of antiretroviral drugs are still needed.

Through a review of different articles, we have identified potential compounds that may have a synergistic effect in combination against HIV-1 infection (Andersen et al. 2019; Ianevski et al. 2019; Andersen et al. 2020).

We tested twelve different combinations of tenofovir with brequinar, suramin, ezetimibe, minocycline, rapamycin, and monensin as well as combinations of lamivudine with the same drugs against HIV-1-mediated firefly luciferase expression in TZM-bl cells. The firefly luciferase open reading frame (ORF) is integrated into the genome of TZM-bl cells under the HIV-1 LTR promoter.

Virus- and mock-infected TZM-bl cells were treated with an increasing concentration of two drugs. Every drug in a combination was added to the cells at six different concentrations

starting from 0 μM (0 μM ; 0, 016 μM ; 0, 08 μM ; 0, 4 μM ; 2 μM ; 10 μM). After 48 h of infection, HIV-induced luciferase expression was measured to determine compound efficiency of drug combinations against HIV-1 infection. Together with this, cell viability was measured in mock-infected cells using CTG assay to determine combinations toxicity.

Based on the experimental results, only two drug combinations, lamivudine-monensin (Figure 8) and tenofovir-monensin (Figure 9), suppressed HIV-1-mediated expression of firefly luciferase without detectable cytotoxicity. Synergy assessment for lamivudine - monensin and tenofovir - monensin combinations were 5.2 and 5.9, correspondingly.

From the conducted experiments, it can be concluded that the lamivudine-monensin and tenofovir-monensin combinations could result in better efficacy and decreased toxicity for the treatment of HIV-1 infection than these drugs alone.

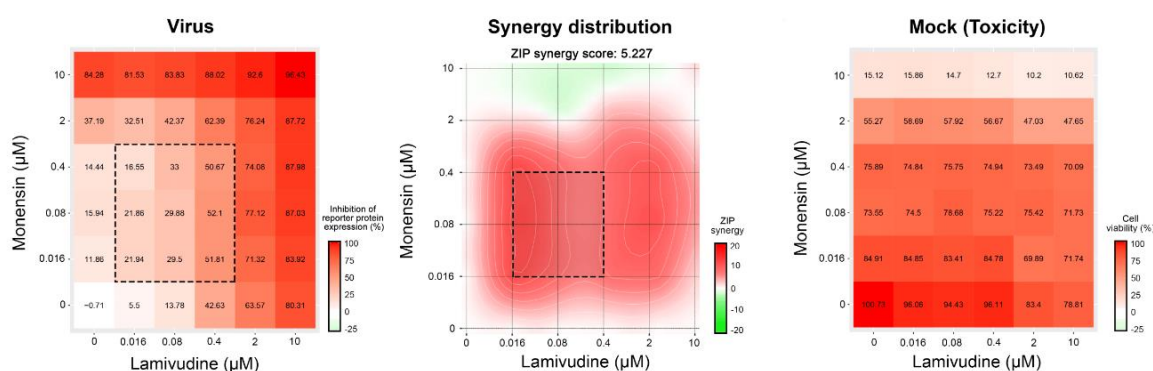


Figure 9 - Monensin and Lamivudine combination landscape. This combination inhibits HIV-1-mediated luciferase expression in TZM-bl cell culture. The left panel shows drugs interaction measured by an HIV-1 virus and TZM-bl cell line expressing luciferase. The right panel depicts Monensin with Lamivudine interaction measured by CTG assay on mock-infected cell culture (modified from (Ianevski, Yao, Biza, et al. 2020)).

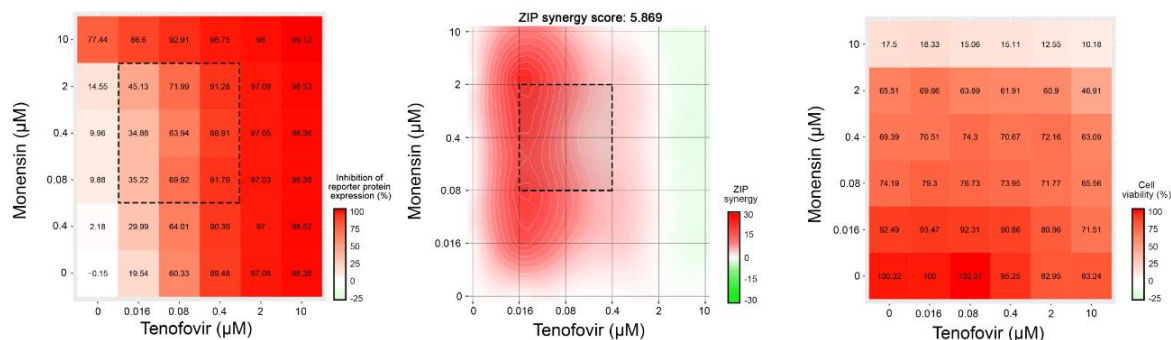


Figure 10 - Monensin and Tenofovir combination landscape. This combination inhibits HIV-1-mediated luciferase expression in TZM-bl cell culture. The left panel shows drugs interaction measured by an HIV-1 virus and TZM-bl cell line expressing luciferase. The right panel depicts Monensin with Tenofovir interaction measured by CTG assay on mock-infected cell culture (modified from (Ianevski, Yao, Biza, et al. 2020)).

3.1.4 Novel antiviral drug combinations against EV1

According to the Baltimore classification, the Picornaviridae family belongs to group IV: viruses with a positive ssRNA strand. This family, according to Viral Zone, is divided into about 35 genera, including the genus Enteroviruses, to which EV1 belongs. The genus Enterovirus is a non-enveloped virus that contains 12 species: rhinovirus A, B, C and enterovirus A, B, C, D, E, F, G, H and J. These viruses cause human diseases such as hand-foot-and-mouth disease (HFMD), common cold, pancreatitis, hemorrhagic conjunctivitis, poliomyelitis, and meningitis. Moreover, Enteroviruses can also be responsible for the chronic cause of diseases like asthma, allergies, and diabetes type I (Diaz-Horta et al. 2012; Jubelt and Lipton 2014).

There are no approved methods for treating and protecting people from enterovirus infections. Moreover, there are no effective antiviral drug combinations against EV1.

To find effective antiviral compounds, the FIMM oncology drug collection was screened (527 drugs) against EV1 in retinal pigment epithelial RPE cells and human cancer lung epithelial A549 using cell viability assay as readout.

As an inhibitor of EV1 replication, we tested vemurafenib. Vemurafenib is an FDA-approved anti-cancer drug for the treatment of people with advanced melanoma. This drug is a competitive kinase inhibitor with activity against B-Raf kinase (B-Raf/MEK/ERK pathway) only if the B-Raf has mutation like V600E (Del Bufalo et al. 2018).

Vemurafenib showed anti-viral replication activity in RPE and A549 cells, which are non-BRAF mutated cells. It means, that this drug does not target BRAF. Most importantly, the experiment shows that vemurafenib can inhibit EV1, but not EV6 (structural identity—88%, similarity—93%) in A549 cells, indicating that it could also affect viral protein (Figure 11).

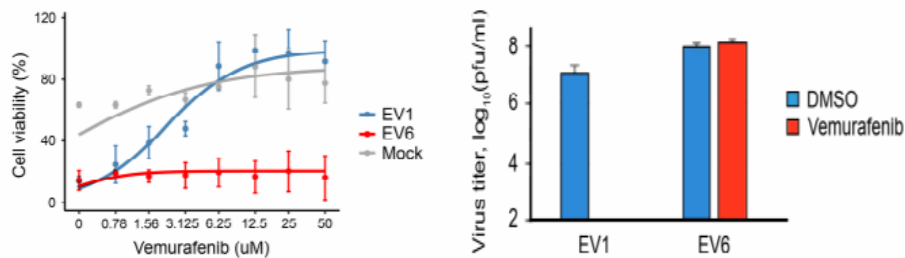


Figure 11- Vemurafenib can inhibit EV1 replication in vitro. Left panel depicts that A549 cells were treated with increasing concentrations of vemurafenib or DMSO and infected with EV1 (moi, 0.1), EV6 (moi, 0.1) or mock. After 24h, the viability of the cells was measured with the CTG assay (mean ± SD; n = 3). Right panel shows that EV1 and EV6 produced in A549 cell line treated with vemurafenib (10 µM) or DMSO was tittered using plaque reduction assay, and the viral titers were rated (mean ± SD; n = 3) (modified from (Ianevski, Yao, Biza, et al. 2020)).

Further, we studied the effect of FDA-approved drug vemurafenib (10 µM) on the metabolism of EV1 (moi 0.1) and mock-infected A549 cell line. After 24 hpi, 90 out of 111 analyzed metabolites were found in cell culture supernatants. It was detected that the level of adenine, adenosine, hypoxanthine, glutathione, NAD, AMP, guanosine, and sucrose are affected by EV1 infection. It is worth noting that vemurafenib showed some impact on the levels of these metabolites as in EV1- and mock-infected A549 cell culture (Figure 12).

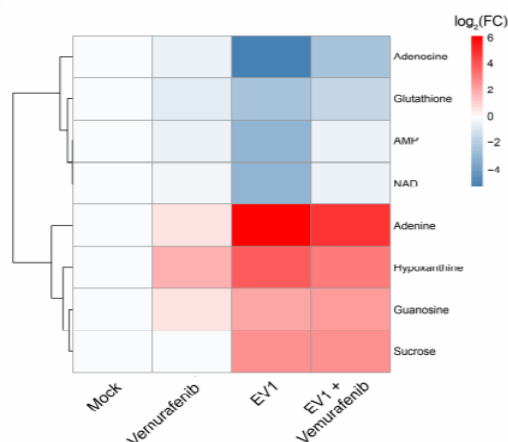


Figure 12 - The level of metabolites changed under EV1 infection and FDA-approved drug Vemurafenib. A549 cell culture was treated with Vemurafenib or non-treated, infected with

EV1 or mock. A map of the most variable metabolites is shown (cut-off: $\log_2FC > 1.5$ and < -1.5). Columns show samples and rows depict metabolites. Each cell is colored according to the \log_2 -transformed values of samples, expressed as fold-change (FC) relative to the average of mock controls. Based on the FC (mean; $n = 3$) metabolites are ranked (modified from (Ianevski, Yao, Biza, et al. 2020)).

After this, the effect of vemurafenib on transcription in viral- and mock-infected cells was identified. A549 cell line was treated with 10 μ M vemurafenib or DMSO and infected with EV1 (moi 0.1) or mock. With help of RNA microarray, via 8 h the expression of cellular genes was analyzed. It was detected that vemurafenib deregulated transcription of some genes in mock and EV1-infected A549 cells (Figure 13). It should be noted that gene set enrichment analysis (GSEA) showed that vemurafenib influenced transcription of 17 cellular genes belonging to GO_RESPONSE_TO_OXYGEN_CONTAINING_COMPOUND and GO_RESPONSE_TO_ENDOGENOUS_STIMULUS gene sets (p-value 9.95 e-15 and 1.24 e-14; FDR q-value 9.45 e-11 and 9.45 e-11). These findings reveal that FDA-approved anti-cancer drug vemurafenib could also target cellular factor(s) which involved in the transcription of antiviral genes.

Next, evaluation of vemurafenib on production of growth factors and cytokines in both virus infected and uninfected A549 cell line was performed. For this, medium from EV1 (moi 0.1) or mock-infected, DMSO- or drug-treated (10 μ M) cells were collected and clarified by centrifugation after 24h. Proteome profiler human cytokine array kit was used to analyze cytokines. Figure 14 depicts how EV1 replication inhibited CXCL-1, PDF-AA, CCL2, IL8, Angiogenin, IGFBP-2, and VEGF expression and activated production of FGF-2, whereas vemurafenib treatment reversed this virus-mediated effect.

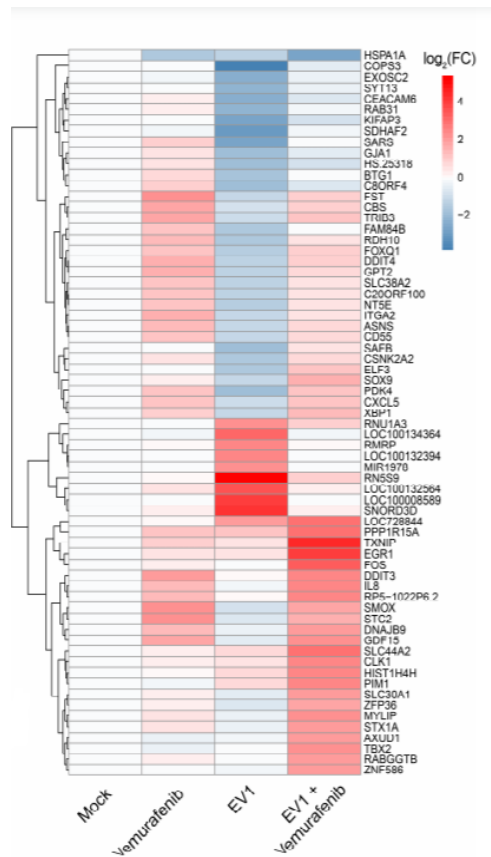


Figure 13 - Vemurafenib effects transcription of EV-1 and mock-infected A549 cells. A549 cell culture was treated with Vemurafenib or non-treated and infected with virus or mock. Via 8 hours post infection, the cells were collected, total RNA was extracted, and gene expression profiling was performed. A map of the most variable genes is depicted (cut-off: $\log_2FC > 1$ and < -1). Columns show treatment and rows depict name of genes. Each cell is colored according to the \log_2 -transformed and quantile-normalized values of the samples, expressed as FC relative to the average of mock controls (modified from (Ianevski, Yao, Biza, et al. 2020)).

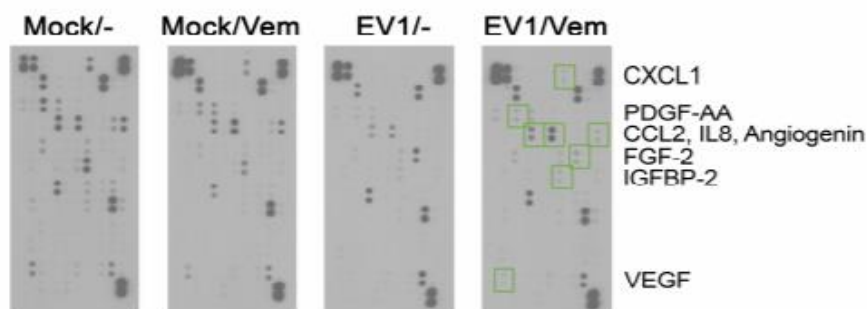


Figure 14 - A549 cell culture was treated with Vemurafenib or non-treated, infected with virus or mock. The cell line media were collected via 24h. Using a human cytokine array, the levels of growth factors, chemokines, cytokines, and other soluble proteins were defined. Dots, corresponding to stricken cytokines, are indicated and scanned array membranes are displayed (modified from (Ianevski, Yao, Biza, et al. 2020)).

Further, combinations of vemurafenib with emetine, homoharringtonine, obatoclox, gemcitabine, or dalbavancin, which are known inhibitors of EV1 infection, were tested (Andersen et al. 2019).

A culture of A549 cells infected with EV1 and mock-infected was treated with increasing concentration of vemurafenib and increasing concentration of a second drug in combination. Compounds were added to the cells at six different concentrations starting from 0 μM (0 μM ; 0, 08 μM ; 0, 04 μM ; 0, 2 μM ; 1 μM ; 5 μM). The viability of mock- and virus-infected A549 cell culture was measured by CTG assay, after 24 hpi (Figure 15).

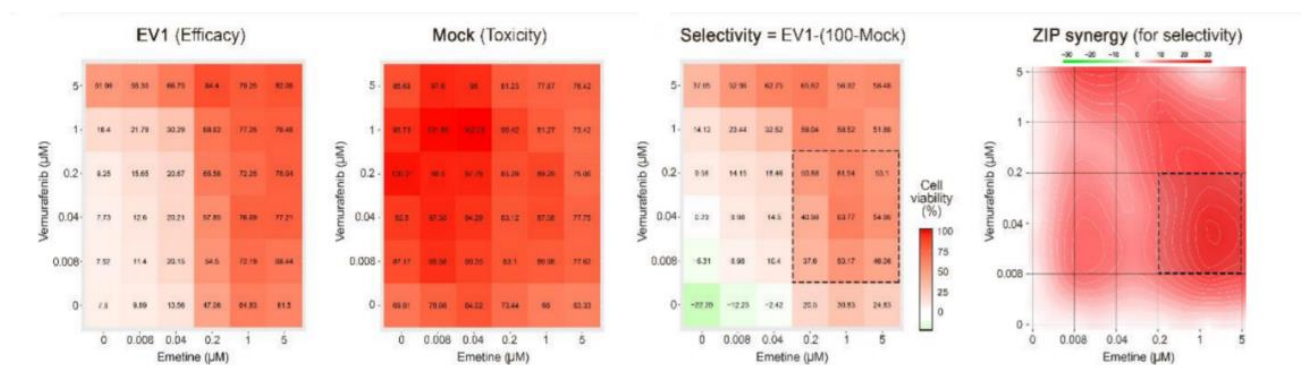


Figure 15 - The representative interaction landscape of vemurafenib and emetine (modified from (Ianevski, Yao, Biza, et al. 2020)).

Synergy score of efficacies (EV1-infected A549 cells) and selectivity (mock infected A549 cells) for drug combinations, considering their toxicity, were calculated (Table 2).

	Efficacy	Selectivity
Vemurafenib + Emetine	9.30	13.38
Vemurafenib + Homoharringtonine	10.44	13.11
Vemurafenib + Gemcitabine	6.37	11.65
Vemurafenib + Obatoclox	5.38	9.85
Vemurafenib + Anisomycin	22.73	30.76
Vemurafenib + Cycloheximide	11.23	18.18

Table 2 - Synergy scores of six antiviral combinations were rated for efficacy and selectivity.

Antiviral combinations of vemurafenib plus emetine, homoharringtonine, gemcitabine, or obatoclox were synergistic (synergy score > 5). However, at selected concentrations, only

vemurafenib-emetine and vemurafenib-homoharringtonine decreased the EV1 production by >2 logs in comparison to vemurafenib alone (Figure 15).

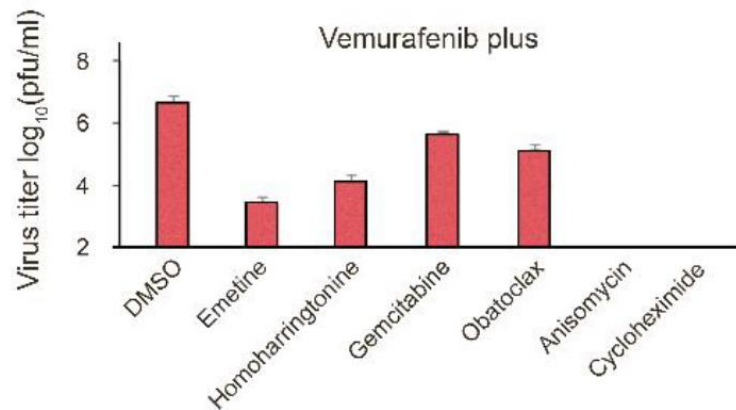


Figure 16 - The effects of vemurafenib plus seven different compounds on EV1 replication measured by plaque reduction assay (modified from (Ianevski, Yao, Biza, et al. 2020)).

Next, anisomycin and cycloheximide were identified as two new antivirals against EV1 infection in vitro. They confirmed their activity in the A549 cell culture (Figure 16).

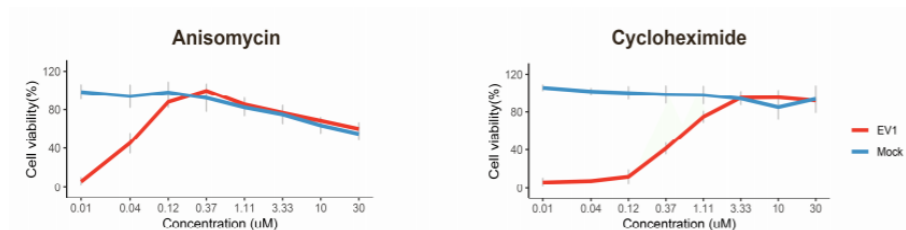


Figure 17 - The A549 cell line was treated with increasing concentrations of Anisomycin (left panel) and Cycloheximide (right panel). This cell culture was infected with the EV1 (moi, 0.1) or mock. Cell viability was measured using CellTiter-Glo assay after 24 hpi. Mean \pm SD; n = 3 (modified from (Ianevski, Yao, Biza, et al. 2020)).

Further, vemurafenib-anisomycin and vemurafenib-cycloheximide combinations were tested against EV1 infection (Figure 17). These combinations were synergistic with synergy score more than 5 (Table 2). It is worth noting that vemurafenib-anisomycin and vemurafenib-cycloheximide combinations reduced the EV1 production by >2 logs in comparison to vemurafenib alone (Figure 15).

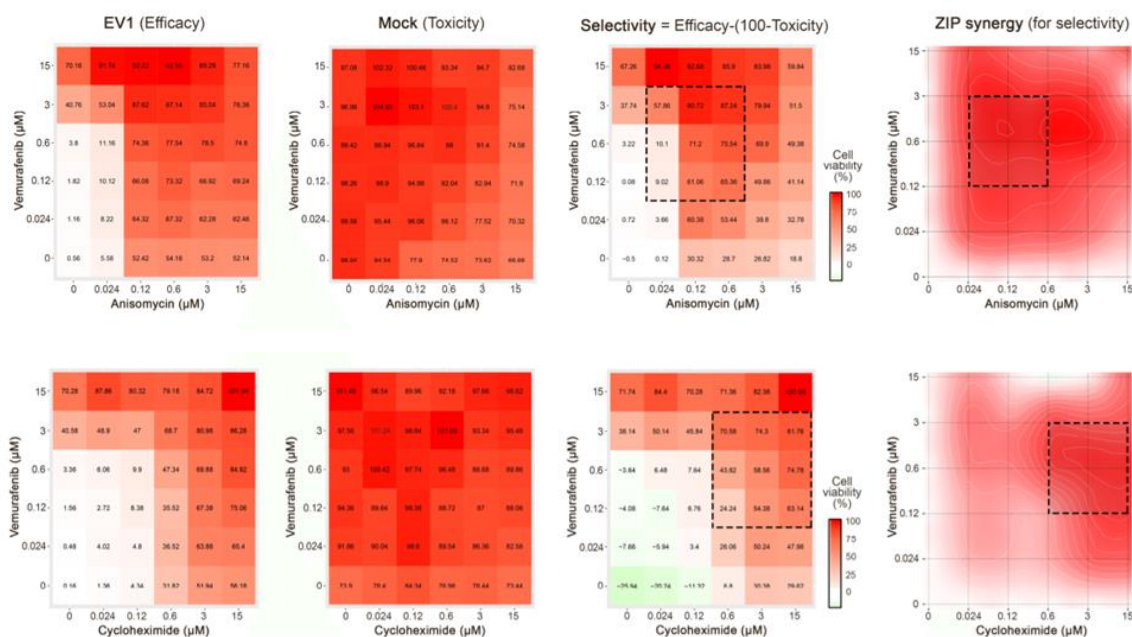


Figure 18 - Vemurafenib-anisomycin and vemurafenib-cycloheximide landscape interaction. Each compound in combination was added to the cells at six different concentrations: 0 μM ; 0,024 μM ; 0,12 μM ; 0,6 μM ; 3 μM ; 15 μM (modified from (Ianevski, Yao, Biza, et al. 2020)).

Thus, vemurafenib was identified as novel antiviral agent against EV-1 infection. This compound showed some impact on the levels of different metabolites: adenine, adenosine, hypoxanthine, glutathione, NAD, AMP, guanosine, and sucrose as in EV1- and mock-infected A549 cells. Also, it was detected that vemurafenib could also target cellular factor(s) which involved in the transcription of antiviral genes. It can be concluded that vemurafenib plus emetine, homoharringtonine, anisomycin or cycloheximide reduced the EV1 in vitro by >2 logs in comparison to vemurafenib alone.

3.2 Results on the development of drug combination database

Until now, research on drug synergy is often disjointed, and there is not a centralized system for generalization and aggregation of synergistic, additive, and antagonistic interactions between antiviral compounds. To solve this problem, we have developed an antiviral drug combination database containing all possible drug combinations with synergistic or additive action against various viruses. In addition, this database includes different states of combinations development: in vitro, in vivo and in clinical trials. (Figure 20). The data of the antiviral drug combinations are posted on the website: <https://antiviralcombi.info/>, which is

freely available for everyone. The website is regularly updated to include new combinations as they become available or to change the status of existing ones as updates become available. In addition, the website also has modules for searching, filtering, visualizing, and loading, which makes the use clearer and more understandable.

The database includes 985 antiviral drug combinations with synergy or additive activity comprising two, three or four drug cocktails. It covers 612 unique drugs and 68 different viruses (Figure 19).

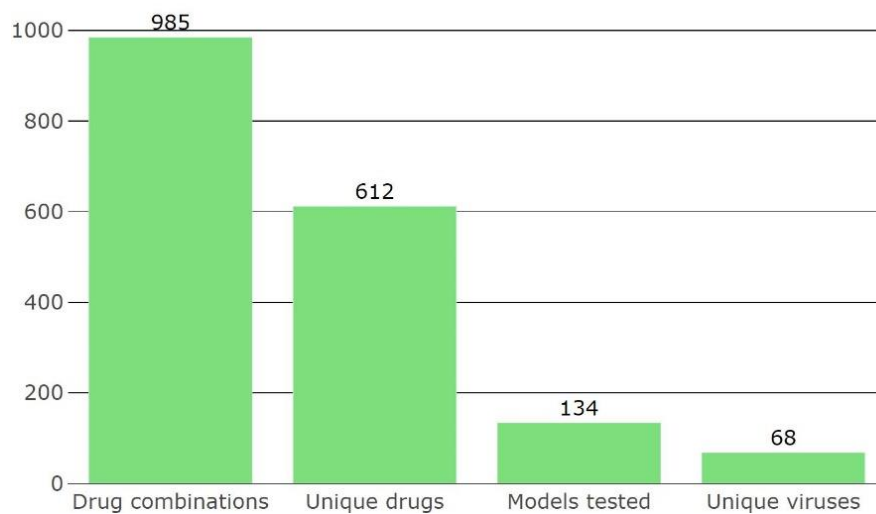


Figure 19 - Database summary table contains information about the overall amount of drug combinations, unique drugs, viruses, and tested models.

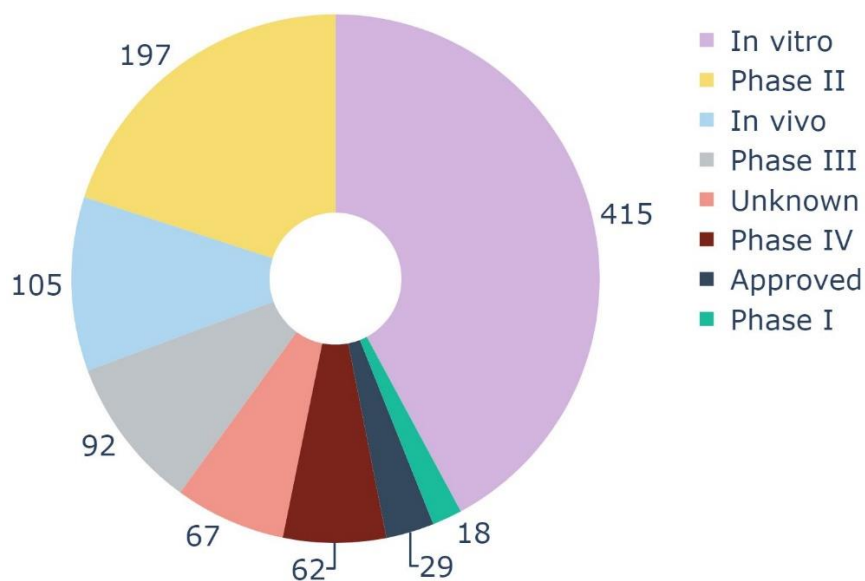


Figure 20 - Developmental phases of combinations that are presented in the database.

Chapter 4

Conclusions and Future Work

4.1 Conclusions

In this thesis, we considered two research problems regarding antiviral drug combinations: experimental investigations and database development. The main goal behind the experiments is to find more effective antiviral drug combinations against SARS-CoV-2, EV1, HIV-1 and HCV infection in vitro. The main goal of the database development is to create a comprehensive database that contains all possible combinations of antiviral drugs with synergistic and additive action against various human viruses.

The experimental results for SARS-CoV-2 infection show that nelfinavir plus convalescent serum, EIDD-2801, remdesivir, salinomycin, amodiaquine, homoharringtonine or obatoclox combinations, as well as the combination of amodiaquine and salinomycin were synergistic with synergy score more than 10 in Calu-3 cells. Also, the amodiaquine-nelfinavir combination was effective against 7 different strains of SARS-CoV-2 infection: S4, S5, S10, S12, S15, E9 and E10. The experimental results for EV1 reveal that vemurafenib with emetine, homoharringtonine, gemcitabine, obatoclox, anisomycin or cycloheximide have synergistic anti-EV1 activity in A549 cells with synergistic score greater than 5. In addition, all combinations, except vemurafenib with gemcitabine or obatoclox, decreased EV1 by more than 2 logs compared to vemurafenib alone. These promising results can help to fight with diseases caused by EV1 infection in the future. The results of experiments on HIV-1 infection show that combinations of monensin with tenofovir or lamivudine have anti-HIV-1 activity with a synergy index greater than 5 in TZM-bl cells. Further, the experimental results for HCV infection reveal that sofosbuvir-brequinar or niclosamide combinations reduce GFP expression in HCV- infected Huh-7.5 cells with synergy scores 24 and 5, respectively.

Experiments suggest that synergy is often achieved when a virus-directed compound is combined with another virus- or host- directed drug. In addition, there is a relatively poor understanding of the mechanisms that leads to synergistic interactions between antiviral compounds. A synergy assessment that is usually performed in a mechanism-unbiased way can help to explain the potentially synergistic combinations even without knowing their mechanisms of actions. Therefore, new drug combinations require further study.

Regarding the database development, we went through all the major sources and databases like PubMed, Web on Science, Scopus, and Google Scholar to find original research manuscripts, review articles, and case reports. We used the main search combinations as “Synergistic” OR “Antiviral” OR “Additive” OR “Combinatorial” AND “Drug Therapy” OR “Drug combinations” OR “Combination drug therapy” OR “Combinations” to create a comprehensive database of all possible combinations of antiviral drugs with synergistic and additive action against human viruses. The database covers 612 unique drugs and 68 different viruses and includes 1008 antiviral drug combinations.

Overall, we identified novel and reviewed known synergistic antiviral combinations against emerging and re-emerging viruses, and we believe that this systematized knowledge will help not only scientists, but also doctors in the tactics of treating and preventing viral infections.

4.2 Future work

The found antiviral drug combinations against SARS-COV-2, HIV-1, HCV and EV1 infection should be further studied to explain the mechanism of their synergy. Thereafter, the synergistic effect should be confirmed in vivo model systems. The results obtained using animal models should then be evaluated at different stages of clinical trials.

Regarding the database development, it should further be updated on a regular basis and synergy data can be used to further explore the most promising and develop the most effective antiviral drug combinations.

References

- Adalja, A., and T. Inglesby. 2019. 'Broad-Spectrum Antiviral Agents: A Crucial Pandemic Tool', *Expert Rev Anti Infect Ther*, 17: 467-70.
- Ali, I., and O. M. L. Alharbi. 2020. 'COVID-19: Disease, management, treatment, and social impact', *Sci Total Environ*, 728: 138861.
- Andersen, P. I., A. Ianevski, H. Lysvand, A. Vitkauskiene, V. Oksenysh, M. Bjørås, K. Telling, I. Lutsar, U. Dumpis, Y. Irie, T. Tenson, A. Kantele, and D. E. Kainov. 2020. 'Discovery and development of safe-in-man broad-spectrum antiviral agents', *Int J Infect Dis*, 93: 268-76.
- Andersen, P. I., K. Krpina, A. Ianevski, N. Shtaida, E. Jo, J. Yang, S. Koit, T. Tenson, V. Hukkanen, M. W. Anthonsen, M. Bjoras, M. Evander, M. P. Windisch, E. Zusinaite, and D. E. Kainov. 2019. 'Novel Antiviral Activities of Obatoclox, Emetine, Niclosamide, Brequinar, and Homoharringtonine', *Viruses*, 11.
- Bailey, J. R., E. Barnes, and A. L. Cox. 2019. 'Approaches, Progress, and Challenges to Hepatitis C Vaccine Development', *Gastroenterology*, 156: 418-30.
- Bauer, D. J. 1985. 'A history of the discovery and clinical application of antiviral drugs', *Br Med Bull*, 41: 309-14.
- Bekerman, E., and S. Einav. 2015. 'Infectious disease. Combating emerging viral threats', *Science*, 348: 282-3.
- Bösl, K., A. Ianevski, T. T. Than, P. I. Andersen, S. Kuivanen, M. Teppor, E. Zusinaite, U. Dumpis, A. Vitkauskiene, R. J. Cox, H. Kallio-Kokko, A. Bergqvist, T. Tenson, A. Merits, V. Oksenysh, M. Bjørås, M. W. Anthonsen, D. Shum, M. Kaarbø, O. Vapalahti, M. P. Windisch, G. Superti-Furga, B. Snijder, D. Kainov, and R. K. Kandasamy. 2019. 'Common Nodes of Virus-Host Interaction Revealed Through an Integrated Network Analysis', *Front Immunol*, 10: 2186.
- Brown, A. J., J. J. Won, R. L. Graham, K. H. Dinnon, 3rd, A. C. Sims, J. Y. Feng, T. Cihlar, M. R. Denison, R. S. Baric, and T. P. Sheahan. 2019. 'Broad spectrum antiviral remdesivir inhibits human endemic and zoonotic deltacoronaviruses with a highly divergent RNA dependent RNA polymerase', *Antiviral Res*, 169: 104541.
- Chaudhuri, S., J. A. Symons, and J. Deval. 2018. 'Innovation and trends in the development and approval of antiviral medicines: 1987-2017 and beyond', *Antiviral Res*, 155: 76-88.
- De Clercq, E., and G. Li. 2016. 'Approved Antiviral Drugs over the Past 50 Years', *Clin Microbiol Rev*, 29: 695-747.
- Del Bufalo, F., G. Ceglie, A. Cacchione, I. Alessi, G. S. Colafati, A. Carai, F. Diomedici-Camassei, E. De Billy, E. Agolini, A. Mastronuzzi, and F. Locatelli. 2018. 'BRAF V600E Inhibitor (Vemurafenib) for BRAF V600E Mutated Low Grade Gliomas', *Front Oncol*, 8: 526.
- Diaz-Horta, O., A. Baj, G. Maccari, A. Salvatoni, and A. Toniolo. 2012. 'Enteroviruses and causality of type 1 diabetes: how close are we?', *Pediatr Diabetes*, 13: 92-9.
- García-Serradilla, M., C. Risco, and B. Pacheco. 2019. 'Drug repurposing for new, efficient, broad spectrum antivirals', *Virus Res*, 264: 22-31.
- Ghosn, J., B. Taiwo, S. Seedat, B. Autran, and C. Katlama. 2018. 'HIV', *Lancet*, 392: 685-97.
- Govorkova, E. A., and R. G. Webster. 2010. 'Combination chemotherapy for influenza', *Viruses*, 2: 1510-29.
- Ianevski, A., P. I. Andersen, A. Merits, M. Bjørås, and D. Kainov. 2019. 'Expanding the activity spectrum of antiviral agents', *Drug Discov Today*, 24: 1224-28.

- Ianevski, A., A. K. Giri, and T. Aittokallio. 2020. 'SynergyFinder 2.0: visual analytics of multi-drug combination synergies', *Nucleic Acids Res*, 48: W488-w93.
- Ianevski, A., L. He, T. Aittokallio, and J. Tang. 2017. 'SynergyFinder: a web application for analyzing drug combination dose-response matrix data', *Bioinformatics*, 33: 2413-15.
- Ianevski, A., R. Yao, S. Biza, E. Zusinaite, A. Mannik, G. Kivi, A. Planken, K. Kurg, E. M. Tombak, M. Ustav, Jr., N. Shtaida, E. Kuleskiy, E. Jo, J. Yang, H. Lysvand, K. Løseth, V. Oksenysh, P. A. Aas, T. Tenson, A. Vitkauskienė, M. P. Windisch, M. H. Fenstad, S. A. Nordbø, M. Ustav, M. Bjørås, and D. E. Kainov. 2020. 'Identification and Tracking of Antiviral Drug Combinations', *Viruses*, 12.
- Ianevski, A., R. Yao, M. H. Fenstad, S. Biza, E. Zusinaite, T. Reisberg, H. Lysvand, K. Løseth, V. M. Landsem, J. F. Malmring, V. Oksenysh, S. E. Erlandsen, P. A. Aas, L. Hagen, C. H. Pettersen, T. Tenson, J. E. Afset, S. A. Nordbø, M. Bjørås, and D. E. Kainov. 2020. 'Potential Antiviral Options against SARS-CoV-2 Infection', *Viruses*, 12.
- Irwin, K. K., N. Renzette, T. F. Kowalik, and J. D. Jensen. 2016. 'Antiviral drug resistance as an adaptive process', *Virus Evol*, 2: vew014.
- Jubelt, B., and H. L. Lipton. 2014. 'Enterovirus/picornavirus infections', *Handb Clin Neurol*, 123: 379-416.
- Khalifa, S. A. M., N. Yosri, M. F. El-Mallah, R. Ghonaim, Z. Guo, S. G. Musharraf, M. Du, A. Khatib, J. Xiao, A. Saeed, H. H. R. El-Seedi, C. Zhao, T. Efferth, and H. R. El-Seedi. 2020. 'Screening for natural and derived bio-active compounds in preclinical and clinical studies: One of the frontlines of fighting the coronaviruses pandemic', *Phytomedicine*: 153311.
- Kim, D. E., J. S. Min, M. S. Jang, J. Y. Lee, Y. S. Shin, J. H. Song, H. R. Kim, S. Kim, Y. H. Jin, and S. Kwon. 2019. 'Natural Bis-Benzylisoquinoline Alkaloids-Tetrandrine, Fangchinoline, and Cepharanthine, Inhibit Human Coronavirus OC43 Infection of MRC-5 Human Lung Cells', *Biomolecules*, 9.
- Lee, M., J. Yang, E. Jo, J. Y. Lee, H. Y. Kim, R. Bartenschlager, E. C. Shin, Y. S. Bae, and M. P. Windisch. 2017. 'A Novel Inhibitor IDPP Interferes with Entry and Egress of HCV by Targeting Glycoprotein E1 in a Genotype-Specific Manner', *Sci Rep*, 7: 44676.
- Lee, M., J. Yang, S. Park, E. Jo, H. Y. Kim, Y. S. Bae, and M. P. Windisch. 2016. 'Micrococcin P1, a naturally occurring macrocyclic peptide inhibiting hepatitis C virus entry in a pan-genotypic manner', *Antiviral Res*, 132: 287-95.
- Loggi, E., R. Vukotic, and P. Andreone. 2018. 'Managing HCV treatment failure and the potential of resistance testing in informing second-line therapy options', *Expert Rev Anti Infect Ther*, 16: 833-38.
- McCluskey, S. M., M. J. Siedner, and V. C. Marconi. 2019. 'Management of Virologic Failure and HIV Drug Resistance', *Infect Dis Clin North Am*, 33: 707-42.
- Melville, K., T. Rodriguez, and H. M. Dobrovolsky. 2018. 'Investigating Different Mechanisms of Action in Combination Therapy for Influenza', *Front Pharmacol*, 9: 1207.
- Musarrat, F., V. Chouljenko, A. Dahal, R. Nabi, T. Chouljenko, S. D. Jois, and K. G. Kousoulas. 2020. 'The anti-HIV drug nelfinavir mesylate (Viracept) is a potent inhibitor of cell fusion caused by the SARSCoV-2 spike (S) glycoprotein warranting further evaluation as an antiviral against COVID-19 infections', *J Med Virol*.
- Naggie, S., and A. J. Muir. 2017. 'Oral Combination Therapies for Hepatitis C Virus Infection: Successes, Challenges, and Unmet Needs', *Annu Rev Med*, 68: 345-58.
- Nijhuis, M., N. M. van Maarseveen, and C. A. Boucher. 2009. 'Antiviral resistance and impact on viral replication capacity: evolution of viruses under antiviral pressure occurs in three phases', *Handb Exp Pharmacol*: 299-320.
- Plempner, R., R. Cox, and J. Wolf. 2020. 'Therapeutic MK-4482/EIDD-2801 Blocks SARS-CoV-2 Transmission in Ferrets', *Res Sq*.

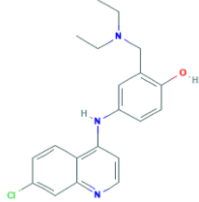
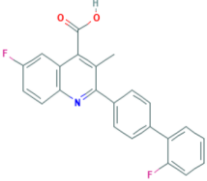
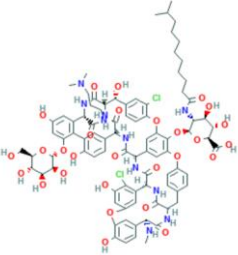
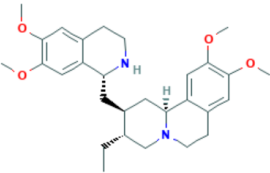
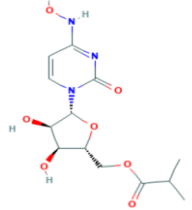
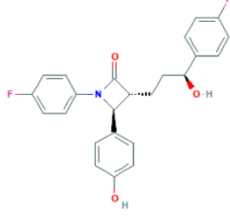
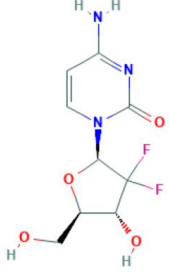
- Potdar, S., A. Ianevski, J. P. Mpindi, D. Bychkov, C. Fiere, P. Ianevski, B. Yadav, K. Wennerberg, T. Aittokallio, O. Kallioniemi, J. Saarela, and P. Östling. 2020. 'Breeze: an integrated quality control and data analysis application for high-throughput drug screening', *Bioinformatics*, 36: 3602-04.
- Ritchie, M. E., B. Phipson, D. Wu, Y. Hu, C. W. Law, W. Shi, and G. K. Smyth. 2015. 'limma powers differential expression analyses for RNA-sequencing and microarray studies', *Nucleic Acids Res*, 43: e47.
- Saag, M. S. 2019. 'HIV 101: fundamentals of antiretroviral therapy', *Top Antivir Med*, 27: 123-27.
- Sheahan, T. P., A. C. Sims, R. L. Graham, V. D. Menachery, L. E. Gralinski, J. B. Case, S. R. Leist, K. Pyrc, J. Y. Feng, I. Trantcheva, R. Bannister, Y. Park, D. Babusis, M. O. Clarke, R. L. Mackman, J. E. Spahn, C. A. Palmiotti, D. Siegel, A. S. Ray, T. Cihlar, R. Jordan, M. R. Denison, and R. S. Baric. 2017. 'Broad-spectrum antiviral GS-5734 inhibits both epidemic and zoonotic coronaviruses', *Sci Transl Med*, 9.
- Siddiqui, A. J., S. Jahan, S. A. Ashraf, M. Alreshidi, M. S. Ashraf, M. Patel, M. Snoussi, R. Singh, and M. Adnan. 2020. 'Current status and strategic possibilities on potential use of combinational drug therapy against COVID-19 caused by SARS-CoV-2', *J Biomol Struct Dyn*: 1-14.
- Smura, T., L. Kakkola, S. Blomqvist, P. Klemola, A. Parsons, H. Kallio-Kokko, C. Savolainen-Kopra, D. E. Kainov, and M. Roivainen. 2013. 'Molecular evolution and epidemiology of echovirus 6 in Finland', *Infect Genet Evol*, 16: 234-47.
- Toots, M., J. J. Yoon, R. M. Cox, M. Hart, Z. M. Sticher, N. Makhsous, R. Plesker, A. H. Barrena, P. G. Reddy, D. G. Mitchell, R. C. Shean, G. R. Bluemling, A. A. Kolykhalov, A. L. Greninger, M. G. Natchus, G. R. Painter, and R. K. Plemper. 2019. 'Characterization of orally efficacious influenza drug with high resistance barrier in ferrets and human airway epithelia', *Sci Transl Med*, 11.
- WHO. 2019. 'HIV/AIDS Overview'.
- . 2020. 'Summary of key facts about HCV', WHO.
- . 2021. 'COVID-19 Weekly Epidemiological Update'.
- Woolhouse, M., F. Scott, Z. Hudson, R. Howey, and M. Chase-Topping. 2012. 'Human viruses: discovery and emergence', *Philos Trans R Soc Lond B Biol Sci*, 367: 2864-71.
- Xie, X., A. E. Muruato, X. Zhang, K. G. Lokugamage, C. R. Fontes-Garfias, J. Zou, J. Liu, P. Ren, M. Balakrishnan, T. Cihlar, C. K. Tseng, S. Makino, V. D. Menachery, J. P. Bilello, and P. Y. Shi. 2020. 'A nanoluciferase SARS-CoV-2 for rapid neutralization testing and screening of anti-infective drugs for COVID-19', *bioRxiv*.
- Zhang, C. H., Y. F. Wang, X. J. Liu, J. H. Lu, C. W. Qian, Z. Y. Wan, X. G. Yan, H. Y. Zheng, M. Y. Zhang, S. Xiong, J. X. Li, and S. Y. Qi. 2005. 'Antiviral activity of cepharanthine against severe acute respiratory syndrome coronavirus in vitro', *Chin Med J (Engl)*, 118: 493-6.

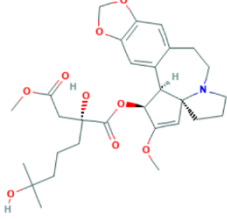
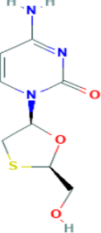
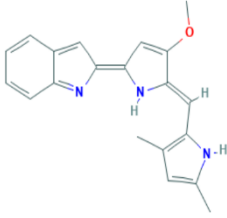
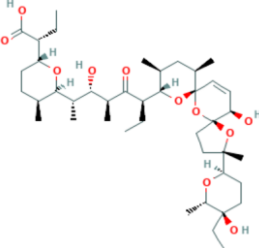

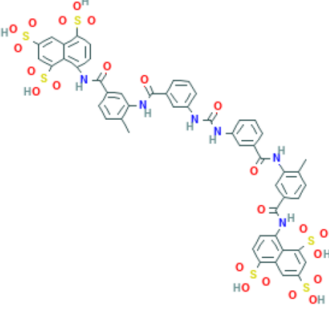
Appendix A – Drugs’ description used in experimental work

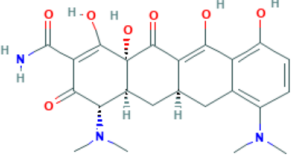
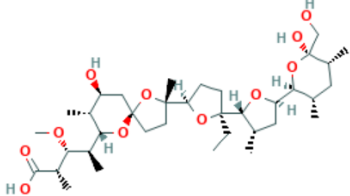
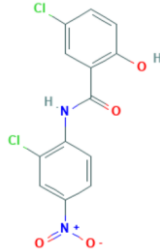
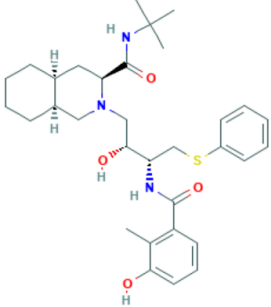
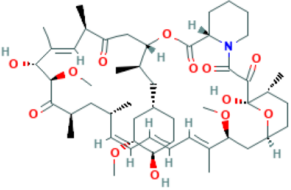
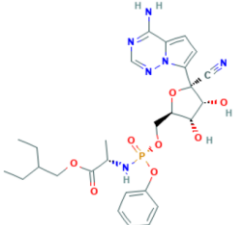
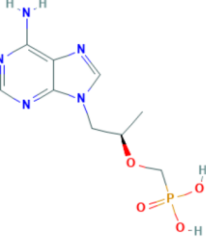
Table A1 - The drugs used in the experiments, their suppliers and catalog numbers.


Drug	CAS	Supplier	Purity (%)	Cat. #	MW	Formula
Amodiaquine	86-42-0	Cayman Chemical	>95	15954	356	C ₂₀ H ₂₂ ClN ₃ O
Brequinar	96187-53-0	Cayman Chemical	>98	24445	375	C ₂₃ H ₁₅ F ₂ N ₂ O ₂
Dalbavancin	171500-79-1	Sigma-Aldrich	>98	SML2378-5MG	1816	C ₈₈ H ₁₀₁ Cl ₃ N ₁₀ O ₂₈
Emetine	7083-71-8	Cayman Chemical	>98	21048	481	C ₂₉ H ₄₀ N ₂ O ₄ ·HCl
Gemcitabine	122111-03-9	Sigma-Aldrich	98	G6423	300	C ₉ H ₁₁ F ₂ N ₃ O ₄ · HCl
Homoharringtonine	26833-87-4	Cayman Chemical	>98	14631	546	C ₂₉ H ₃₉ N ₉ O
Lamivudine	134678-17-4	Selleckchem	>99	S1706	229	C ₈ H ₁₁ N ₃ O ₃ S
Obatoclox	803712-79-0	MedChemExpress	99,7	HY-10969	413,49	C ₂₁ H ₂₃ N ₃ O ₄ S
Salinomycin	53003-10-4	MedChem Express	≥98	HY-15597	751	C ₄₂ H ₇₀ O ₁₁
Sofosbuvir	1190307-88-0	MedChemExpress	100	HY-15005	530	C ₂₂ H ₂₉ F ₃ N ₃ O ₉ P
Suramin	129-46-4	Acros	98	328540500	1297	C ₅₁ H ₄₀ N ₆ O ₂₃ S ₆
Minocycline	13614-98-7	Cayman Chemical	>98	CAYM14454	458	C ₂₃ H ₂₇ N ₃ O ₇ HCl
Monensin	22373-78-0	Cayman Chemical	≥98	16488	671	C ₃₆ H ₆₁ O ₁₁ · Na
Niclosamide	50-65-7	Dr. Ehrenstorfer	97	C15510000	327	C ₁₃ H ₈ Cl ₂ N ₂ O ₄
Nelfinavir	159989-65-8	Cayman Chemical	>98	15144	664	C ₃₂ H ₄₅ N ₃ O ₄ SCH ₃ SO ₃ H
Rapamycin	53123-88-9	Fisher scientific	>98	BP2963	914	C ₅₁ H ₇₉ N ₁₃
Remdesivir	1809249-37-3	Cayman	>98	30354	602,6	C ₂₇ H ₃₅ N ₆ O ₈ P
Tenofovir	202138-50-9	Acros Organics	98	461250010	636	C ₁₉ H ₃₀ N ₅ O ₁₀ P C ₄ H ₄ O ₄
Vemurafenib	918504-65-1	MedChemExpress	99,8	HY-12057	490	C ₂₃ H ₁₈ ClF ₂ N ₃ O ₃ S

Table A2 - Chemical structure of compounds used in experiments taken from PubChem

Compound	Primary indication	Chemical structure (Source: PubChem)
Amodiaquine	Approved antimalarial	
Brequinar	Investigational anticancer	
Dalbavancin	Approved antibacterial	
Emetine	Approved antiprotozoal	
EIDD-2801	Experimental	
Ezetimibe	Approved lipid-lowering	
Gemcitabine	Approved anticancer	

Homoharringtonine	Approved anticancer	
Lamivudine	Approved antiviral	
Obatoclax	Investigational anticancer	
Salinomycin	Approved antibacterial	
Sofosbuvir	Approved antiviral	
Suramin	Approved antiprotozoal	

Minocycline	Approved	
Monensin	Approved antibacterial	
Niclosamide	Approved antihelminthic	
Nelfinavir	Approved antiviral	
Rapamycin	Approved immunosuppressant	
Remdesivir	Approved	
Tenofovir	Approved antiviral	

Vemurafenib	Approved	 <p>The image shows the chemical structure of Vemurafenib. It consists of a central indazole ring system. One nitrogen atom in the indazole ring is bonded to a hydrogen atom. The 3-position of the indazole ring is substituted with a 4-chlorophenyl group. The 4-position of the indazole ring is substituted with a 2,6-difluorophenyl group. The 5-position of the indazole ring is substituted with a propylsulfonamide group (-NH-SO₂-CH₂-CH₂-CH₃).</p>
--------------------	----------	---

Appendix B – Antiviral drug combinations database

Due to the size of the created table database, it is attached to the thesis as a separate file. Below, other supportive information is provided.

Table B1 - Full name of viruses included in the database, their abbreviated name, which family they belong to which structure of the genetic material they have and what diseases can cause.

Virus	Abbreviation	Family	Group	Viral disease
Adenovirus	ADV	Adenoviridae	dsDNA	Acute respiratory disease
BK virus	BKV	Polyomaviridae	dsDNA	Nephropathy and hemorrhagic cystitis
Chikungunya virus	CHIKV	Togaviridae	(+)ssRNA	Chikungunya fever
Coxsackievirus B3	CVB3 (HEV-B)	Picornaviridae	(+)ssRNA	Viral myocarditis
Crimean–Congo hemorrhagic fever virus	CCHFV	Nairoviridae	(-)ssRNA	Crimean–Congo hemorrhagic fever
Cytomegalovirus	CMV	Herpesviridae	dsDNA	Mononucleosis-like illness*
Dengue virus	DENV	Flaviviridae	(+)ssRNA	Dengue fever
Ebola virus	EBOV	Filoviridae	(-)ssRNA	Ebola hemorrhagic fever
Echovirus 1	EV1 (HEV-B)	Picornaviridae	(+)ssRNA	Febrile illness and aseptic meningitis
Echovirus 6	EV6 (HEV-B)	Picornaviridae	(+)ssRNA	Neurological symptoms, aseptic meningitis
Enterovirus 70	EV70 (HEV-D)	Picornaviridae	(+)ssRNA	Acute hemorrhagic conjunctivitis
Enterovirus 71	EV71 (HEV-A)	Picornaviridae	(+)ssRNA	Hand, foot, and mouth disease
Epstein-Barr virus	EBV	Herpesviridae	dsDNA	Infectious mononucleosis
Hepatitis B virus	HBV	Hepadnaviridae	dsDNA-RT	Hepatitis B
Hepatitis C virus	HCV	Flaviviridae	(+)ssRNA	Hepatitis C
Hepatitis D virus	HDV	Unassigned	(-)ssRNA	Hepatitis D
Hepatitis E virus	HEV	Hepeviridae	(+)ssRNA	Hepatitis E
Herpes simplex virus 1	HSV-1	Herpesviridae	dsDNA	Cold sores
Herpes simplex virus 2	HSV-2	Herpesviridae	dsDNA	Genital herpes
Human herpesvirus 6	HHV-6	Herpesviridae	dsDNA	Exanthema subitum
Human immunodeficiency virus 1	HIV-1	Retroviridae	ssRNA-RT	Acquired immune deficiency syndrome
Human immunodeficiency virus 2	HIV-2	Retroviridae	ssRNA-RT	Acquired immune deficiency syndrome
Human metapneumovirus	HMPV	Pneumoviridae	(-)ssRNA	Lower respiratory infection in young children
Human papillomavirus	HPV	Papillomaviridae	dsDNA	Genital warts and laryngeal papillomatosis
Human rhinovirus A2	HRV2 (HRV-A)	Picornaviridae	(+)ssRNA	Cold-like illnesses
Influenza A virus	FLUAV	Orthomyxoviridae	(-)ssRNA	Influenza
Influenza B virus	FLUBV	Orthomyxoviridae	(-)ssRNA	Influenza
Japanese encephalitis virus	JEV	Flaviviridae	(+)ssRNA	Japanese encephalitis
John Cunningham virus	JCV	Polyomaviridae	dsDNA	Progressive multifocal leukoencephalopathy

Junin virus	JUNV	Arenaviridae	(-)ssRNA	Argentine hemorrhagic fever
Kaposi's sarcoma-associated herpesvirus	KSHV	Herpesviridae	dsDNA	Kaposi's sarcoma
Lassa virus	LASV	Arenaviridae	(-)ssRNA	Lassa hemorrhagic fever
Marburg virus	MARV	Filoviridae	(-)ssRNA	Marburg hemorrhagic fever
Middle East respiratory syndrome coronavirus	MERS-CoV	Coronaviridae	(+)ssRNA	Middle East respiratory syndrome
Molluscum contagiosum virus	MCV	Poxviridae	dsDNA	Molluscum contagiosum
Norovirus	NoV	Caliciviridae	(+)ssRNA	Gastroenteritis
Parvovirus B19	B19V	Parvoviridae	ssDNA	Erythema infectiosum
Poliovirus	PV (HEV-C)	Picornaviridae	(+)ssRNA	Poliomyelitis
Rabies virus	RABV	Rhabdoviridae	(-)ssRNA	Rabies
Respiratory syncytial virus	RSV	Pneumoviridae	(-)ssRNA	Lower respiratory tract infections
Rift Valley fever virus	RVFV	Phenuiviridae	(-)ssRNA	Rift Valley fever
Rotavirus	RV	Reoviridae	dsRNA	Gastroenteritis
Severe acute respiratory syndrome coronavirus	SARS-CoV	Coronaviridae	(+)ssRNA	Severe acute respiratory syndrome
Severe acute respiratory syndrome coronavirus 2	SARS-CoV-2	Coronaviridae	(+)ssRNA	Severe acute respiratory syndrome
Severe fever with thrombocytopenia syndrome virus	SFTSV	Phenuiviridae	(-)ssRNA	Severe fever with thrombocytopenia syndrome
Sindbis virus	SINV	Togaviridae	(+)ssRNA	Rash and arthritis
Tick-borne encephalitis virus	TBEV	Flaviviridae	(+)ssRNA	Tick-borne encephalitis
Vaccinia virus	VACV	Poxviridae	dsDNA	No disease in human
Varicella zoster virus	VZV	Herpesviridae	dsDNA	Chickenpox (varicella)
Vesicular stomatitis virus	VSV	Rhabdoviridae	(-)ssRNA	Vesicular stomatitis
West Nile virus	WNV	Flaviviridae	(+)ssRNA	West Nile fever
Yellow fever virus	YFV	Flaviviridae	(+)ssRNA	Yellow fever
Zika virus	ZIKV	Flaviviridae	(+)ssRNA	Zika virus disease
Coxsackievirus A16	FMDV (HEV-A)	Picornaviridae	(+)ssRNA	Hand, foot, and mouth disease

